


 Cite this: *RSC Adv.*, 2020, 10, 15107

Positive effects of concomitant heavy metals and their redoxates on hexavalent chromium removal in microbial fuel cells†

 Xiayuan Wu,^a Chunrui Li,^a Zuopeng Lv,^b Xiaowei Zhou,^c Zixuan Chen,^a Honghua Jia,^a Jun Zhou,^a Xiaoyu Yong,^a Ping Wei^a and Yan Li^{*a}

Cr(VI) laden wastewaters generally comprise a range of multiple heavy metals such as Au(III) and Cu(II) with great toxicity. In the present study, cooperative cathode modification by biogenic Au nanoparticles (BioAu) reduced from aqueous Au(III) and *in situ* Cu(II) co-reduction were investigated for the first time to enhance Cr(VI) removal in microbial fuel cells (MFCs). With the co-existence of Cu(II) in the catholyte, the MFC with carbon cloth modified with nanocomposites of multi-walled carbon nanotubes blended with BioAu (BioAu/MWCNT) obtained the highest Cr(VI) removal rate ($4.07 \pm 0.01 \text{ mg L}^{-1} \text{ h}^{-1}$) and power density ($309.34 \pm 17.65 \text{ mW m}^{-2}$), which were 2.73 and 3.30 times as high as those for the control, respectively. The enhancements were caused by BioAu/MWCNT composites and deposited redoxates of Cu(II) on the cathode surface, which increased the adsorption capacity, electronic conductivity and electrocatalytic activity of the cathode. This study provides an alternative approach for efficiently remediating co-contamination of multiple heavy metals and simultaneous bioenergy recovery.

Received 15th February 2020

Accepted 5th April 2020

DOI: 10.1039/d0ra01471k

rsc.li/rsc-advances

1. Introduction

Hexavalent chromium (Cr(VI)), typically found in industrial wastewaters such as electroplating and mining wastewaters due to widespread industrial application, is a known extremely toxic heavy metal to living organisms.¹ Microbial fuel cells (MFCs) have recently shown promising results for recovering various heavy metals from wastewaters in addition to simultaneous organic wastewater treatment and bioelectricity generation.^{2–4} In particular, the electrochemical reduction of Cr(VI) in MFCs has been reported in the literature with variable degrees of success through the optimization of operation conditions, reactor architectures and cathode electrodes.^{5–10} However, the non-conductive Cr(III) deposits reduced from Cr(VI) on the cathode surface led to severe cathode deactivation, exerting negative effects on the electrochemical behavior of the cathode electrode.^{6,10–12} Therefore, it should be put more efforts on *ex situ* or *in situ* improving the electronic conductivity and electrocatalytic activity of the cathode electrode for Cr(VI) reduction.

High concentration of Cr(VI) is usually found together with multiple heavy metal ions (*e.g.* Au(III), Cu(II)) in the acidic wastewaters from the electroplating and mining industries.¹³ On the other hand, chemical Au nanoparticles as electrode modifiers, especially decorating other nanomaterials such as multi-walled carbon nanotubes (MWCNTs), can significantly improve the electrochemical reduction of Cr(VI).¹⁴ Biogenic Au nanoparticles (BioAu), which can be recovered from wastewaters containing Au(III) ions by microorganisms such as *Shewanella oneidensis*, have been reported to possess higher electronic conductivity and electrocatalytic activity compared to the chemical counterpart.^{15,16} Our previous work has demonstrated BioAu/MWCNT modification for the anode remarkably enhanced power output of MFCs.¹⁶ However, the BioAu/MWCNT nanohybrids modified electrode, to our best knowledge, has never been attempted to use as the cathode to reduce Cr(VI) in MFCs. Consequently, BioAu/MWCNT modification might be an *ex situ* strategy to improve the electrochemical properties of the cathode for Cr(VI) reduction, which is certainly warranted further investigations.

Regarding to the *in situ* strategy for improving the Cr(VI)-reducing cathode performance, we hypothesized that some co-existing heavy metals could exert positive effects due to their conductive redoxates deposited on the cathode surface. For example, previous studies have confirmed that the main product of Cu(II) reduction in MFC cathode (pH = 2.2–3.4) was pure Cu.^{3,17} Since Cu possesses excellent conductivity and electrocatalytic activity, the interaction of cathode materials with *in situ* deposited Cu from Cu(II) reduction becomes crucial

^aCollege of Biotechnology and Pharmaceutical Engineering, Nanjing Tech University, No. 30 Puzhu Road(S), Nanjing 211816, Jiangsu, China. E-mail: liyan@njtech.edu.cn; Fax: +86 25 58139929; Tel: +86 25 58139929

^bThe Key Laboratory of Biotechnology for Medicinal Plants of Jiangsu Province, Jiangsu Normal University, Xuzhou 221116, China

^cDepartment of Philosophy, Nanjing University, Nanjing 210023, China

† Electronic supplementary information (ESI) available. See DOI: 10.1039/d0ra01471k



for the improved electrochemical properties of electrodes. The *in situ* deposition of Cu onto the cathode has been demonstrated to efficiently enhance continuous Cu(II) reduction, subsequent Cd(II) reduction as well as energy recovery. Furthermore, different cathode materials influenced the diversity of shapes and morphology of the deposited Cu, resulting in different active surface areas, and consequently the overall performance of MFCs.¹⁷ Therefore, it would be reasonably expected that the co-existence of Cu(II) with Cr(VI) in catholyte might mitigate the cathode deactivation and thereby facilitate Cr(VI) reduction in MFCs. These effects have not been systematically investigated in literatures, especially when interacting with the BioAu/MWCNT modified electrode. Besides, the use of reduction products from Au(III) and Cu(II) to facilitate Cr(VI) reduction is not trivial since Au(III) and Cu(II) often co-exist with Cr(VI) in electroplating and mining wastewaters.

This study aimed to promote the efficiency of Cr(VI) removal in MFCs through *ex situ* and *in situ* improving the electrochemical properties of the cathode. The effects of cooperative cathode modification by BioAu/MWCNT nanohybrids and *in situ* Cu(II) co-reduction on Cr(VI) removal in MFCs were systematically investigated. The performance of MFCs was evaluated in terms of cathodic Cr(VI) and Cu(II) removal, anodic COD removal as well as electricity generation. The precipitations on the cathode surface after operation were defined by scanning electron microscopy with coupled energy dispersive spectroscopy (SEM-EDS) and X-ray photoelectron spectroscopy (XPS). This work reveals a new insight into the way to combat poisonous Cr(VI) through other poisonous heavy metals co-existing in wastewaters.

2. Materials and methods

2.1. Fabrication of cathode electrode

An unmodified carbon cloth (25 cm², Shanghai Hesun, China) was set as the bare electrode.¹⁶ As described in our previous work,¹⁶ BioAu (spherical, 5–15 nm in size) was synthesized by *S. oneidensis* MR-1 reducing aqueous Au(III) (ESI, Fig. S1†). BioAu and MWCNT powder paste was prepared according to the procedures in our previous study.¹⁶ Subsequently, this paste was evenly spread on a 50% polytetrafluoroethylene (PTFE) carbon cloth.¹⁶ The modified carbon cloth was washed thrice with distilled water to remove the unadsorbed BioAu/MWCNT. After drying at 105 °C, the BioAu/MWCNT electrode was fabricated. When the BioAu loading amount was set at 0.83 ± 0.02 mg cm⁻², different BioAu/MWCNT ratios (1 : 0, 1 : 1, 1 : 2) were investigated to optimize the electrode fabrication; afterwards, the BioAu/MWCNT ratio was set at 1 : 2, different BioAu loading amounts (0.40 ± 0.01, 0.83 ± 0.02, 1.84 ± 0.01 mg cm⁻²) were investigated as well.

2.2. Construction and operation of MFC

The MFC was assembled by two identical cubic chambers with an effective volume of 70 mL as described previously.¹⁶ In order to keep the pH difference intact, a bipolar membrane (38.5 cm², Beijing Yanrun, China) was applied to separate the anode and

cathode chambers.^{13,18} The anode electrode was a graphite felt (25 cm², Hunan Jiuhua, China), and the cathode electrode was a bare or modified carbon cloth. The stable bioanode was acclimatized in advance by inoculating anaerobic digester sludge.¹⁹ The anolyte was artificial wastewater containing a buffering solution (1 g L⁻¹ glucose and 50 mM phosphate, pH 7.0).¹⁶ The catholyte, unless specified, was 50 mM phosphate buffer solution (PBS) containing 100 mg L⁻¹ Cr(VI) (K₂Cr₂O₇ solution) at pH 2.5. The MFCs were operated in a batch-fed mode (25 ± 0.5 °C) with an external resistance of 1000 Ω, unless specified. In order to ensure reproducibility, all MFC reactors were conducted in triplicate.

2.3. Effects of co-existing Cu(II) in catholyte

The effects of co-existing Cu(II) on Cr(VI) removal were studied through adding 400 mg L⁻¹ Cu(II) (CuSO₄·5H₂O solution) into the MFC catholyte mentioned above. In this case, the MFCs with the bare and BioAu/MWCNT electrode in the presence of Cu(II) were dubbed the “Bare-CrCu” and “BioAu/MWCNT-CrCu” MFC, respectively. Meanwhile, the MFCs for removing sole Cr(VI) (100 mg L⁻¹) and sole Cu(II) (400 mg L⁻¹) were carried out to serve as the corresponding control groups. Hence, the MFCs with two different electrodes for sole Cr(VI) and sole Cu(II) removal were denoted as the “Bare-Cr”, “BioAu/MWCNT-Cr”, “Bare-Cu” and “BioAu/MWCNT-Cu” MFC. In this section, all experimental MFCs were connected to an external resistance of 10 Ω. The Cr(VI)/Cu(II) concentration ratio (1 : 4) and external resistance (10 Ω) were chosen based on the optimization experimental results shown in ESI (Fig. S2 and S3†).

2.4. Analytical methods

The voltage, power density, and internal resistance of MFCs were obtained according to the methods described in our previous work.¹⁹ Cyclic voltammetry (CV) and electrochemical impedance spectroscopy (EIS) were used to evaluate the electrochemical characteristics of the electrodes. CV was tested in a three-electrode system (reference electrode: Ag/AgCl electrode, working electrode: tested electrode, counter electrode: Pt electrode) as previously described.¹⁶ The electrolyte for CV test was 10 mM PBS (pH = 7). EIS analysis was performed with the same three-electrode system (frequency range: 100 kHz to 5 mHz, potential amplitude: 10 mV) in the electrolyte consisting of 5 mM K₃Fe(CN)₆ and 0.2 M KCl (pH = 7).

SEM-EDS (Hitachi S-4800, Japan) was used to analyze the morphology and element contents of the electrode surface. The specific surface area (SSA), contact-angle, and surface resistance of the electrode were characterized as previously described.¹⁹ The elemental compositions of the precipitates on the cathode surface after operation were detected by X-ray photoelectron spectroscopy (XPS, PHIQuantera II, Japan).

The concentrations of soluble Cr(VI) and chemical oxygen demand (COD) were determined by using the standard methods.²⁰ The soluble Cu(II) concentration was analyzed by atomic absorption spectroscopy (WFX-130, Beijing Ruili Analytical Instrument Co. Ltd., China). The MFC experiments lasted for 24 h, and the catholyte sampling was conducted on



0 h, 2 h, 4 h, 6 h, 8 h, 24 h for soluble Cr(vi) and Cu(II) concentration analyses.

3. Results and discussion

3.1. Effects of BioAu/MWCNT ratio and BioAu loading amount on electrode

In order to obtain the suitable BioAu/MWCNT ratio for electrode modification, effects of different BioAu/MWCNT ratios (1 : 0, 1 : 1, 1 : 2) on electrochemical characteristics of the carbon cloth were investigated when the BioAu loading amount was set at $0.83 \pm 0.02 \text{ mg cm}^{-2}$. The electrochemical characteristics of different electrodes before operation were evaluated through measuring CV and EIS (Fig. 1). As shown in Fig. 1A, there were no peaks in the CV curves of all the electrodes since no redox reactions happened in PBS. Whereas, there is a significant increase in current range of each modified electrode compared with that of the bare electrode, suggesting that the modified carbon cloths had a higher faradaic charge capacity and electron transfer efficiency possibly due to the physico-chemical properties of the modifiers. Obviously, the larger proportion of MWCNT powder occupied in the modifier, the higher faradaic current was observed in CV. The highest current range was found in the electrode with the BioAu/MWCNT ratio of 1 : 2, indicating that MWCNTs were favorable supports for BioAu modification because of their unique electrical and structural properties.²¹ Anchoring of metal nanoparticles over MWCNTs is an effective strategy in improving the dispersion of nanoparticles, which increases the electrochemically available surface area and electrocatalytic active sites of electrodes.²² Similar synergistic effects have also been found in other nanocomposite modification studies using MWCNTs blending with metal nanoparticles such as TiO_2 , Fe_3O_4 , and SnO_2 .^{21,23,24}

Furthermore, the interfacial electrochemical properties of modified electrodes were also evaluated by EIS.²⁵ Fig. 1B shows the Nyquist plots of all the electrodes. The x-intercept of a Nyquist plot represents R_s , and the semicircle diameter indicates R_{ct} . There were no distinct differences in R_s of all the electrodes, whereas all the electrodes presented significant differences in the observed R_{ct} . The R_{ct} decreased with the increased proportion of MWCNT powder in the modifiers, signifying remarkable enhancements of the catalytic reaction and electron transfer efficiency at the electrodes with the addition of MWCNTs. Accordingly, the electrode with the BioAu/MWCNT ratio of 1 : 2 possessed the smallest R_{ct} . The EIS results were in good agreement with the CV results.

As the BioAu/MWCNT ratio was set at 1 : 2, effects of different BioAu loading amounts (0.40 ± 0.01 , 0.83 ± 0.02 , $1.84 \pm 0.01 \text{ mg cm}^{-2}$) on the electrochemical characteristics of the carbon cloth were studied as well. Similarly, the larger BioAu loading amount caused the higher faradaic current range of the CV curve (Fig. 1C), indicating that BioAu possessed the ability to facilitate electron transfer on the electrode. The largest BioAu loading amount ($1.84 \pm 0.01 \text{ mg cm}^{-2}$) achieved the best electrochemical performance for the electrode. EIS analysis (Fig. 1D) further confirmed that the larger BioAu loading

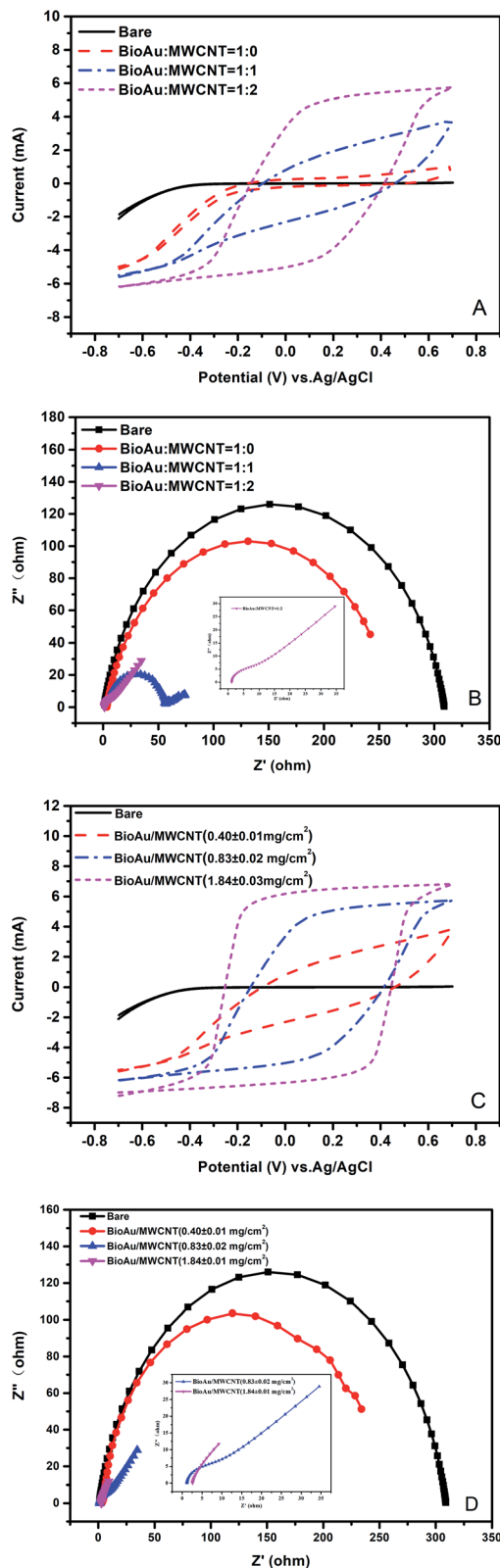


Fig. 1 CV and EIS analysis of electrodes with different BioAu/MWCNT ratios (A and B) and different BioAu loading amounts (C and D) before operation.



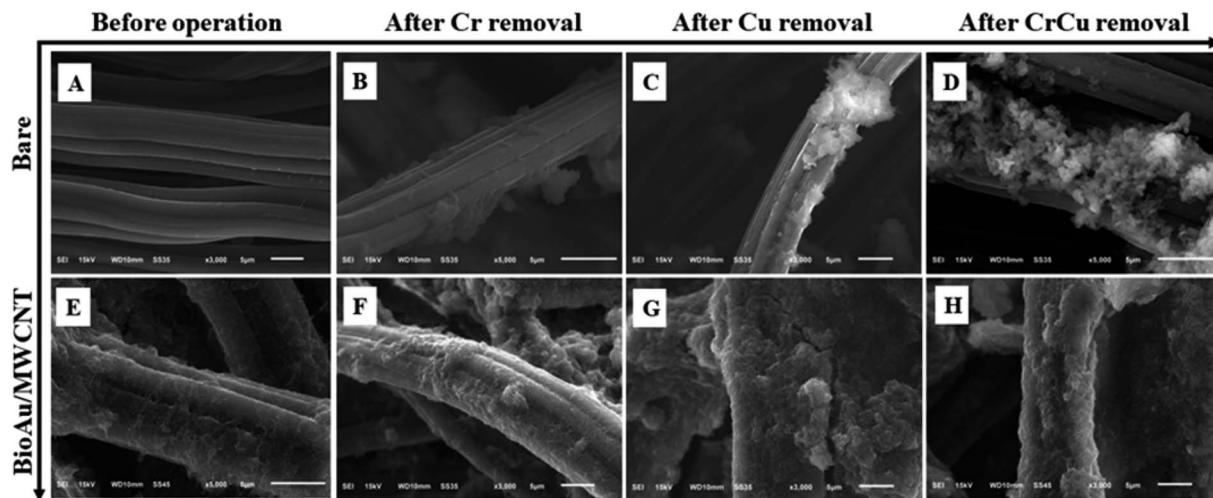


Fig. 2 SEM images of the bare (A–D) and BioAu/MWCNT ((E–H) BioAu/MWCNT ratio: 1 : 2, BioAu loading amount: $1.84 \pm 0.01 \text{ mg cm}^{-2}$) electrode before and after operation.

Table 1 Surface characteristics of the bare and BioAu/MWCNT (BioAu/MWCNT ratio: 1 : 2, BioAu loading amount: $1.84 \pm 0.01 \text{ mg cm}^{-2}$) electrode

Electrode	BET SSA ($\text{m}^2 \text{g}^{-1}$)	Contact angle ($^\circ$)	Resistance (Ω)
Bare	3.78 ± 0.34	110.4 ± 0.6	7.5 ± 0.7
BioAu/MWCNT	66.97 ± 0.23	48.2 ± 0.7	6.31 ± 0.9

amount correspondingly reduced the R_{ct} of the modified electrode. Alatraktchi *et al.*²⁶ also proposed that higher Au nanoparticle density led to higher power generation when Au nanoparticle modified carbon papers were applied as anodes in MFCs. Therefore, the BioAu/MWCNT ratio and BioAu loading amount were respectively set at 1 : 2 and $1.84 \pm 0.01 \text{ mg cm}^{-2}$ for the electrode modification in the subsequent experiments.

The surface morphology of the bare and BioAu/MWCNT electrode was observed using SEM-EDS before operation (Fig. 2A and E). Compared with a smooth and clean surface of the bare electrode (Fig. 2A), there were substantial deposits with typical MWCNTs evenly attached on the BioAu/MWCNT electrode (Fig. 2E), resulting in a rougher and more crosslinked surface.²⁷ Au element was detected on the BioAu/MWCNT electrode by EDS, implying the successful modification of BioAu/MWCNT composites on the carbon cloth (ESI, Fig. S4†).

Table 1 presents surface characteristics of the two different electrodes. The SSA value of the BioAu/MWCNT electrode ($66.97 \pm 0.23 \text{ m}^2 \text{g}^{-1}$) was 17.72 times as high as that of the bare electrode ($3.78 \pm 0.34 \text{ m}^2 \text{g}^{-1}$), further confirming that BioAu/MWCNT composites gave rise to a larger surface area. The large surface area can facilitate rapid mass transfer and increase active reaction sites on materials.²⁸ Besides, the BioAu/MWCNT electrode (contact angle: $48.2 \pm 0.7^\circ$) was much more hydrophilic than the bare electrode (contact angle: $110.4 \pm 0.6^\circ$). This was opposite to the BioPd modification results in another study.²⁹ The materials with strong hydrophilicity could have faster electrochemical reactions due to the enhanced mass

transfer on the solid–liquid interface.³⁰ In terms of the surface resistance, the BioAu/MWCNT electrode had a lower value than the bare electrode.

3.2. Electrode performance in Cr(vi)-reducing MFC

Fig. 3 shows the performance of the Cr(vi)-reducing MFCs with the bare and BioAu/MWCNT electrode as cathodes. The voltage output (Fig. 3A) continuously descended as running time in both MFCs. This was mainly caused by the change of Cr(vi) concentration and typically happened in Cr(vi)-reducing MFCs.^{12,31} The maximum voltage output of the MFC with the BioAu/MWCNT electrode achieved 525.01 mV, which was 1.48 times as high as that of the MFC with the bare electrode (354.30 mV). As shown in Fig. 3B, the MFC with the BioAu/MWCNT electrode accordingly produced a maximum power density of $138.38 \pm 6.36 \text{ mW m}^{-2}$, which was around 1.32 times as high as that of the MFC with the bare electrode ($104.99 \pm 4.99 \text{ mW m}^{-2}$). From Fig. 3C, the lower internal resistance was also observed in the MFC with the BioAu/MWCNT electrode ($194.43 \pm 25.39 \Omega$) compared to that in the MFC with the bare electrode ($305.05 \pm 30.04 \Omega$).

MWCNTs have been widely used to remove aqueous metal ions such as Cr(vi) due to the excellent adsorption performance.³² In addition, MWCNTs decorated with chemical Au nanoparticles have also been applied for Cr(vi) detection because of their good electron transfer ability and electrocatalytic activity.¹⁴ Therefore, in order to define the adsorption and electrochemical reduction functions for Cr(vi) removal, each Cr(vi)-reducing MFC was operated with and without circuit connected (Fig. 3D). After 24 h open-circuit operation, the Cr(vi) removal rate in the MFC with the BioAu/MWCNT electrode reached $0.66 \pm 0.04 \text{ mg L}^{-1} \text{ h}^{-1}$ after 24 h, while the MFC with the bare electrode achieved $0.31 \pm 0.02 \text{ mg L}^{-1} \text{ h}^{-1}$. The Cr(vi) removal mechanism under open-circuit condition was mainly the electrode adsorption, indicating that BioAu/MWCNT modification increased the adsorption amounts of aqueous



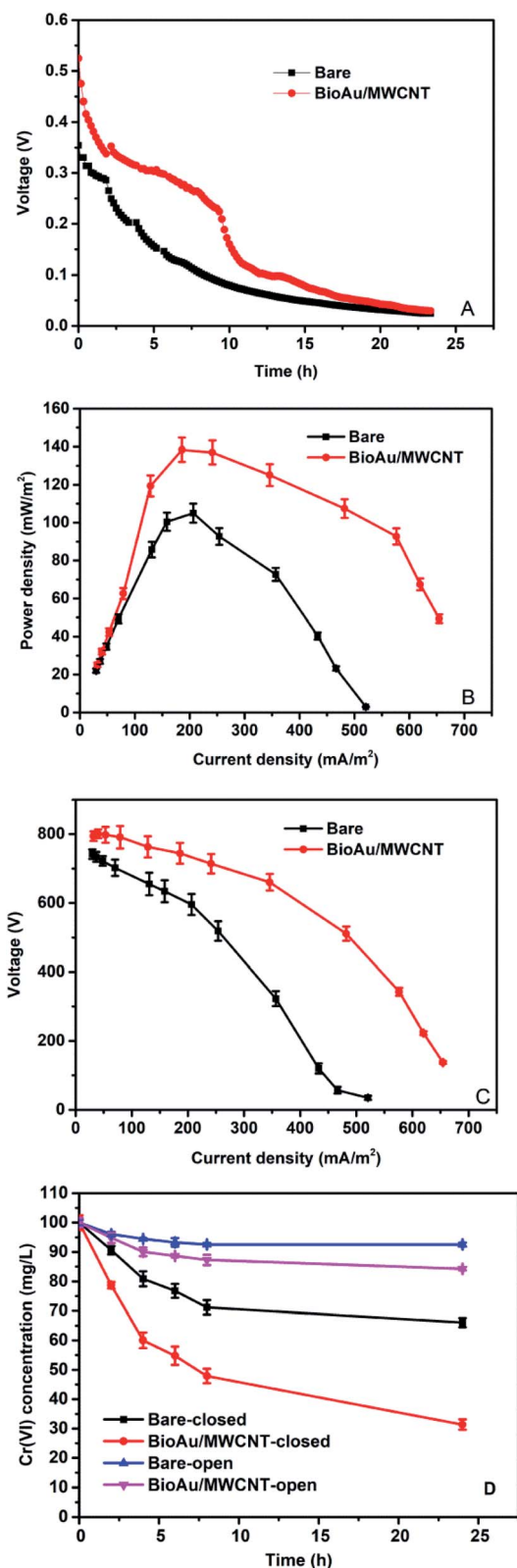


Fig. 3 Voltage outputs (A), power densities (B), polarization curves (C), and dissolved Cr(VI) concentration changes (D) of Cr(VI)-reducing MFCs with different cathode electrodes.

Cr(VI). Clearly, the Cr(VI) removal remarkably enhanced during closed-circuit operation in both MFCs: extra Cr(VI) of 52.93% was further removed in the MFC with the BioAu/MWCNT electrode compared with only 26.50% in the MFC with the bare electrode once the circuit connected, demonstrating that BioAu/MWCNT composites facilitated Cr(VI) electrochemical reduction. The Cr(VI) removal rate of the MFC with the BioAu/MWCNT electrode ($2.86 \pm 0.03 \text{ mg L}^{-1} \text{ h}^{-1}$) was 2.01 times as high as that in the MFC with the bare electrode ($1.42 \pm 0.04 \text{ mg L}^{-1} \text{ h}^{-1}$). Table 2 presents the comparative data of studies on abiotic Cr(VI) reduction in similar two-chamber MFCs. Gangadharan *et al.*⁵ and Gupta *et al.*⁶ respectively investigated a liquid crystal polaroid glass electrode (LCPGE) and an alumina/nickel nanoparticles-dispersed carbon nanofiber electrode (AA: Ni-ACF/CNF) for Cr(VI) removal in MFCs, and the Cr(VI) removal rates in these works were lower than that in the present work (Table 2). The results suggest that the excellent adsorption capacity and electrochemical activity of BioAu/MWCNT composites on the cathode electrode enhanced the power output and Cr(VI) removal in the MFC.

3.3. Effects of co-existing Cu(II) in catholyte

The effects of co-existing Cu(II) (400 mg L^{-1}) on Cr(VI) removal in MFCs with different cathode electrodes were studied at an external resistance of 10Ω (Fig. 4). As shown in Fig. 4A, all the MFCs with the BioAu/MWCNT electrode produced higher voltage outputs than the MFCs with the bare electrode. In particular, the co-existing Cu(II) in catholyte further enhanced the electricity generation of MFCs. The maximum voltage (59.33 mV) was observed from the BioAu/MWCNT-CrCu MFC, which was 2.28 times as high as that of the bare-Cr (26.04 mV) MFC. Table 3 displays the maximum power densities, internal resistances and anodic COD removal of all the MFCs. Clearly, the BioAu/MWCNT-CrCu MFC obtained the highest power density of $309.34 \pm 17.65 \text{ mW m}^{-2}$, which was 1.44 and 3.30 times as high as that of the BioAu/MWCNT-Cr ($215.39 \pm 21.21 \text{ mW m}^{-2}$) and bare-Cr ($93.82 \pm 4.79 \text{ mW m}^{-2}$) MFC, respectively, illustrating the role of Cu(II) in promoting the Cr(VI)-reducing MFCs performance. The co-existing Fe(III) (150 mg L^{-1}) has also been reported to have a synergistic effect on Cr(VI) removal in MFCs, but the current density was only increased by 27.27% compared with that in the absence of Fe(III).² Accordingly, the BioAu/MWCNT-CrCu MFC possessed the lowest internal resistance ($124.42 \pm 9.54 \Omega$), while the bare-Cr MFC had the highest one ($259.52 \pm 21.65 \Omega$). The anodic COD removal reached $79.66 \pm 4.87\%$ in the BioAu/MWCNT-CrCu MFC, which was increased by 78.69% compared to that in the bare-Cr MFC ($44.58 \pm 2.57\%$).

As seen from Fig. 4B, Cr(VI) was removed more quickly in the MFCs with co-existing Cu(II) than MFCs without co-existing Cu(II). The BioAu/MWCNT-CrCu MFC obtained the highest Cr(VI) removal rate ($4.07 \pm 0.01 \text{ mg L}^{-1} \text{ h}^{-1}$), which was 1.36 and 2.73 times as high as that from the BioAu/MWCNT-Cr ($3.00 \pm 0.02 \text{ mg L}^{-1} \text{ h}^{-1}$) and bare-Cr ($1.49 \pm 0.02 \text{ mg L}^{-1} \text{ h}^{-1}$) MFC, respectively, implying that the presence of Cu(II) accelerated the electrochemical reduction of Cr(VI) in MFCs. In addition, the





Table 2 Comparison of studies on abiotic Cr(vi) reduction in two-chamber MFCs^a

No.	Anode (A)/Cathode (C) material	Initial Cr(vi) (mg L ⁻¹) and pH	Other metals (mg L ⁻¹) in catholyte	Power density (mW m ⁻²)	Cr(vi) removal rate (mg L ⁻¹ h ⁻¹)	Reference
1	Graphite plate (A/C)	200, 2.0	None	150	1.06	7
2	Graphite plate (A)/rutile-coated graphite plate (C)	26, 2.0	None	NA	0.97	8
3	Graphite felt (A)/PPy/AQS-modified graphite felt (C)	20, 7.0	None	299.6	0.43	9
4	LCPGE (A/C)	100, 2.0	None	10	2.08	5
5	AA-Ni-ACF/CNF (A/C)	200, 2.0	None	1540	2.13	6
6	Carbon fiber felt (A/C)	250, 2.0	V(v), 250	970.2	0.79	10
7	Graphite felt (A)/carbon rod (C)	50, 1.5	Fe(III), 150	225	9.4	2
8	Graphite felt (A)/BioAu/MWCNT modified carbon cloth (C)	100, 2.5	Cu(II), 400	309.34	4.07	This study

^a NA: not applicable; PPy: polypyrrole; AQS: 9,10-anthraquinone-2-sulfonic acid sodium salt; LCPGE: liquid crystal polarized glass electrode; AA: Ni-ACF/CNF: alumina/nickel nanoparticles-dispersed carbon nanofiber; BioAu/MWCNT: biogenic Au nanoparticles/multi-walled carbon nanotubes.

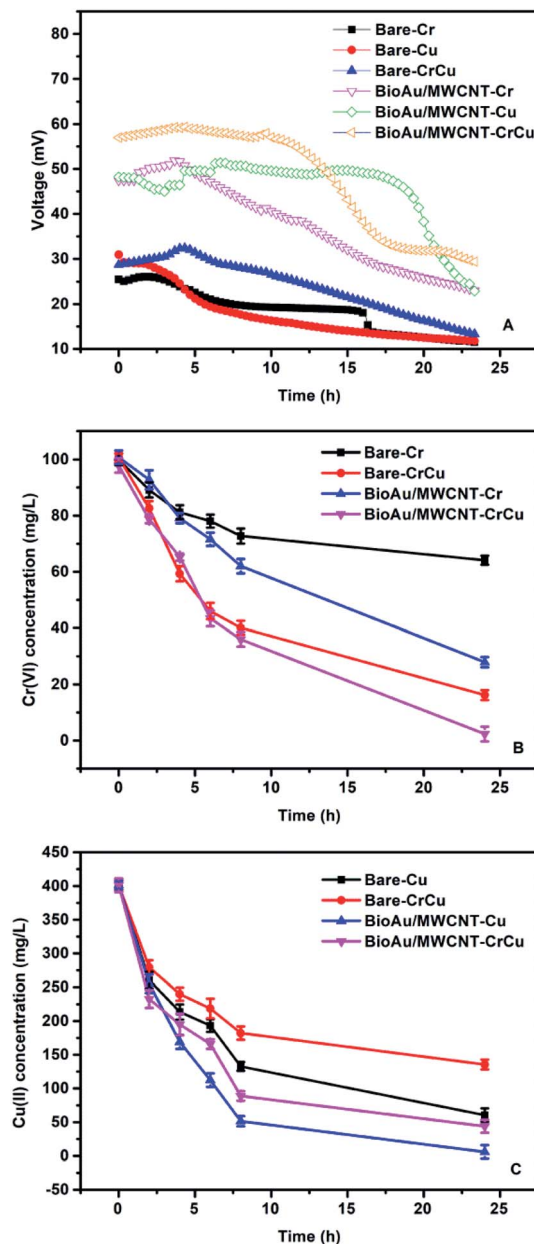


Fig. 4 Voltage outputs (A), dissolved Cr(vi) concentration changes (B), and dissolved Cu(II) concentration changes (C) of MFCs with different cathode electrodes for different heavy metals removal.

enhancement exhibited an increasing trend with the increased Cu(II) concentrations (from 50 mg L⁻¹ to 400 mg L⁻¹) and with the decreased external resistances (from 2000 Ω to 10 Ω), implying more Cu(II) ions and electrons were needed to exert synergistic effects of the co-existing Cu(II) for Cr(vi) reduction (ESI, Fig. S2 and S3†). According to Table 2, although it might not be appropriate to directly compare the Cr(vi) removal efficiency due to different conditions applied in the studies, it still clearly shows that the present study obtained a noticeably higher Cr(vi) removal rate than other studies, except Wang *et al.*'s² study. In their study, a lower pH (1.5) along with the presence of Fe(III), an efficient electron mediator, were used to obtain a higher Cr(vi) removal rate (9.4 mg L⁻¹ h⁻¹) but a lower

Table 3 Maximum power densities (P_{\max}), internal resistances, and anodic COD removal of different MFCs

Group	P_{\max} (mW m ⁻²)	Internal resistance (Ω)	COD removal (%)
Bare-Cr	93.82 \pm 4.79	259.52 \pm 21.65	44.58 \pm 2.57
Bare-Cu	80.03 \pm 5.01	239.17 \pm 26.745	53.21 \pm 1.67
Bare-CrCu	143.60 \pm 12.46	202.09 \pm 18.64	57.64 \pm 3.58
BioAu/MWCNT-Cr	215.39 \pm 21.21	197.64 \pm 17.55	68.65 \pm 2.93
BioAu/MWCNT-Cu	231.38 \pm 13.53	162.32 \pm 13.86	70.91 \pm 1.76
BioAu/MWCNT-CrCu	309.34 \pm 17.65	124.42 \pm 9.54	79.66 \pm 4.87

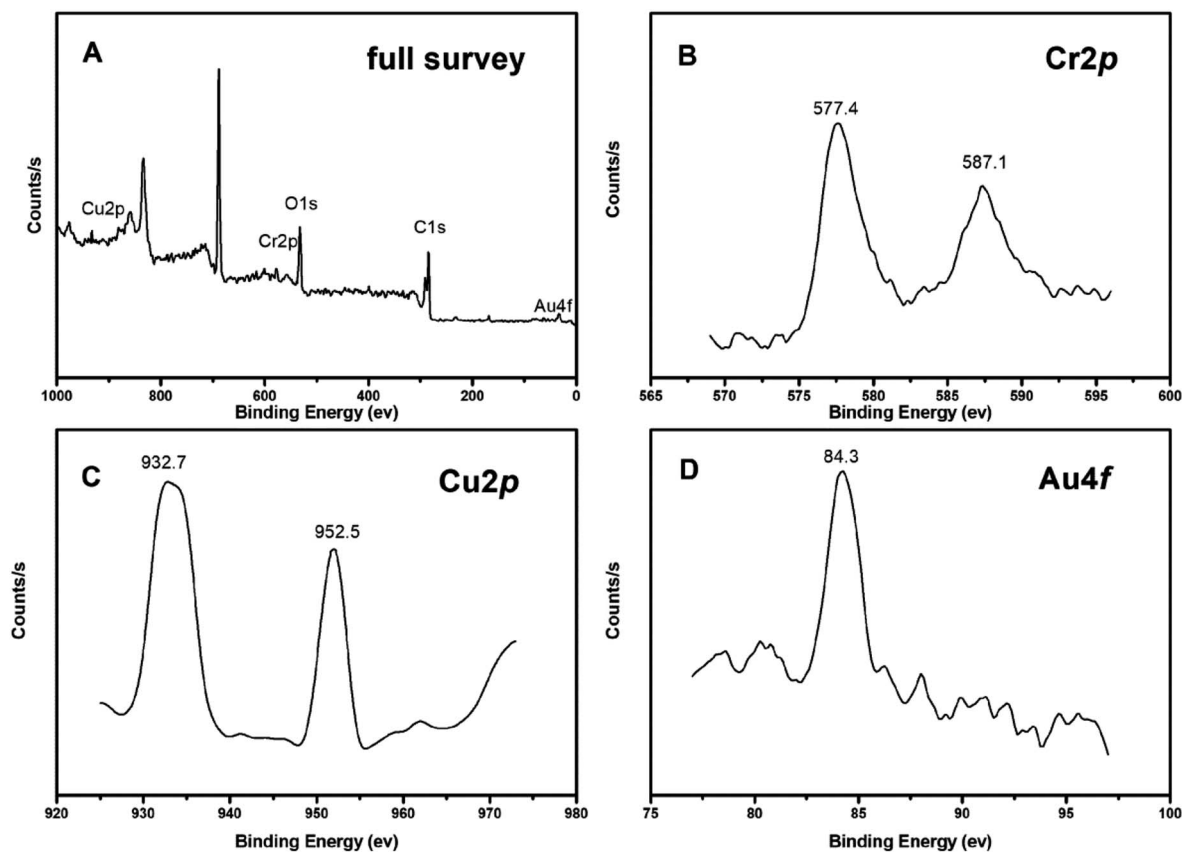


Fig. 5 XPS analysis for the deposits on the BioAu/MWCNT electrode after Cr(VI) and Cu(II) removal ((A) full survey, (B) Cr2p, (C) Cu2p, (D) Au4f).

power density (225 mW m⁻²) than those in our study.² As seen in Fig. 4C, Cu(II) was simultaneously removed with Cr(VI) from catholyte in MFCs, although the Cu(II) removal was slightly lower than that in MFCs with Cu(II) acting as the sole electron acceptor. The Cu(II) removals in the BioAu/MWCNT-CrCu and bare-CrCu MFC reached 89.10 \pm 0.23% and 66.23 \pm 0.98%, respectively, while those in the BioAu/MWCNT-Cu and bare-Cu MFC were 98.54 \pm 0.48% and 84.93 \pm 0.47%. This indicated that BioAu/MWCNT modification could also facilitate Cu(II) removal and the co-existing Cr(VI) negatively affected Cu(II) reduction due to the non-conductive deposits generated from Cr(VI) reduction on the cathode surface.¹⁰ On the other hand, the deposited products of Cu(II) reduction on the cathode appreciably increased the conductivity throughout the cathode electrode, leading to the improved electricity generation and Cr(VI) removal.¹⁷

The bare and BioAu/MWCNT electrode were observed by SEM after 24 h-operation time (Fig. 2). Compared with the corresponding electrodes before operation, some noticeable precipitates were generated on all of the electrode surfaces. In particular, the largest amount of precipitates was found on the BioAu/MWCNT electrode for Cr(VI) and Cu(II) removal (Fig. 2H). This was consistent with the substantial reduction of Cr(VI) and Cu(II) in MFCs (Fig. 4). The BioAu/MWCNT electrode for Cr(VI) and Cu(II) removal was further analyzed by XPS to determine the elemental compositions of precipitates on the surface (Fig. 5). The XPS results showed the presence of Cr, Cu, C, O and Au signals (Fig. 5A). Detailed XPS scans of the Cr2p region (Fig. 5B) were observed Cr2p_{1/2} and Cr2p_{3/2} lines at 577.4 and 587.1 eV, respectively, confirming Cr(VI) was electrochemically reduced to Cr(III) and recovered as Cr₂O₃. Similarly, Cu2p_{3/2} and Cu2p_{1/2} lines at 932.7 and 952.5 eV were respectively observed in Cu2p region



(Fig. 5C), demonstrating that the reduction products of Cu(II) were Cu and Cu₂O. Tao *et al.*³³ reported the same results about Cu(II) reduction products in MFCs. Au4f_{7/2} line at 84.3 eV in Au4f region (Fig. 5D) together with SEM-EDS results proved the successful modification of BioAu/MWCNT composites on the electrode. Previous studies have found that non-conductive Cr(III) deposits on the electrode from Cr(VI) reduction (*e.g.* Cr₂O₃) led to severe cathode deactivation, decreasing electrode conductivity and impeding electron transfer on the cathode.^{5,6,10,13} Due to the cathode deactivation, the Cr(VI) has been demonstrated to negatively affect the co-existing V(V) reduction in MFCs.¹⁰ This phenomenon was similar with the decreased efficiency of co-existing Cu(II) reduction in this study. On the contrary, the deposited products from Cu(II) reduction on the electrode surface have been proven to significantly improve the adsorption capacity, electronic conductivity and electrochemical activity of the cathode, which facilitated the subsequent cycles of Cu(II) and Cd(II) reduction and energy recovery.^{3,17} Moreover, Devaraj *et al.*³⁴ observed a remarkable enhancement of electrochemical activity for the carbon-based electrode after Cu@Cu₂O/MWCNT modification. Therefore, BioAu/MWCNT modification coupling with *in situ* Cu(II) co-reduction noticeably enhanced Cr(VI) removal as well as electricity production in MFCs by improving electrochemical properties of the cathode. Since in practice Cr(VI) laden wastewaters generally comprise a range of multiple heavy metal ions such as Au(III) and Cu(II), this study provides a feasible approach through recovering some heavy metals from wastewaters as *ex situ* or *in situ* electrode modifiers to accelerate Cr(VI) removal. It could simultaneously realize the concomitant heavy metals remediation along with bioenergy generation. However, there are a variety of impurities in the real wastewaters, including not only diverse metal ions but also organic contaminants, which might have different effects on the performance of Cr(VI)-reducing MFCs. For example, except Au(III) and Cu(II), the other co-existing metal ions which might have positive or negative effects on the Cr(VI) removal still need to further investigate. In addition, the interaction effects of metal ions and organic contaminants in the real wastewaters are another subject deserved to study as well. These should be clarified before the application for the real wastewaters in the future.

4. Conclusions

In this study, cooperative cathode modification by biogenic nano-Au reduced from Au(III) and *in situ* Cu(II) co-reduction was used to enhance Cr(VI) removal in MFCs. The highest Cr(VI) removal rate ($4.07 \pm 0.01 \text{ mg L}^{-1} \text{ h}^{-1}$) and power density ($309.34 \pm 17.65 \text{ mW m}^{-2}$) were obtained in the BioAu/MWCNT-CrCu MFC, which were 2.73 and 3.30 times as high as those in the Bare-Cr MFC, respectively. Au(III) and Cu(II) are frequently detected with Cr(VI) in wastewaters from electroplating and mining industries, this study shed a light on positive effects of concomitant heavy metals and their redox states on mitigating the cathode deactivation in Cr(VI)-reducing MFCs.

Conflicts of interest

There are no conflicts of interest to declare.

Acknowledgements

This work was financially supported by the National Key R & D Program of China (2018YFA0902200), the National Natural Science Foundation of China (21808108, 21676142, 51708264), the Natural Science Foundation of Jiangsu Province (BK20180702), the Natural Science Foundation of the Jiangsu Higher Education Institutions of China (18KJB610007), Qing Lan Project of Jiangsu Universities, Six Talent Peaks Project in Jiangsu Province, the Jiangsu Synergetic Innovation Center for Advanced Bio-Manufacture, and the European Union's Horizon 2020 Research and Innovation Programme (GREENER, GA 826312).

References

- 1 W. Jin, H. Du, S. Zheng and Y. Zhang, *Electrochim. Acta*, 2016, **191**, 1044–1055.
- 2 Q. Wang, L. Huang, Y. Pan, X. Quan and G. Li Puma, *J. Hazard. Mater.*, 2017, **321**, 896–906.
- 3 Q. Wang, L. Huang, Y. Pan, P. Zhou, X. Quan, B. E. Logan and H. Chen, *Bioresour. Technol.*, 2016, **200**, 565–571.
- 4 C. Choi and N. Hu, *Bioresour. Technol.*, 2013, **133**, 589–598.
- 5 P. Gangadharan, I. M. Nambi and J. Senthilnathan, *Bioresour. Technol.*, 2015, **195**, 96–101.
- 6 S. Gupta, A. Yadav and N. Verma, *Chem. Eng. J.*, 2017, **307**, 729–738.
- 7 G. Wang, L. Huang and Y. Zhang, *Biotechnol. Lett.*, 2008, **30**, 1959–1966.
- 8 Y. Li, A. Lu, H. Ding, S. Jin, Y. Yan, C. Wang, C. Zen and X. Wang, *Electrochem. Commun.*, 2009, **11**, 1496–1499.
- 9 Y. Pang, D. Xie, B. Wu, Z. Lv, X. Zeng, C. Wei and C. Feng, *Synth. Met.*, 2013, **183**, 57–62.
- 10 B. Zhang, C. Feng, J. Ni, J. Zhang and W. Huang, *J. Power Sources*, 2012, **204**, 34–39.
- 11 N. Xafenias, Y. Zhang and C. J. Banks, *Environ. Sci. Technol.*, 2013, **47**, 4512–4520.
- 12 D. Wu, Z. Huang, K. Yang, D. Graham and B. Xie, *Environ. Sci. Technol.*, 2015, **49**, 4122–4128.
- 13 C. Kim, C. R. Lee, Y. E. Song, J. Heo, S. M. Choi, D.-H. Lim, J. Cho, C. Park, M. Jang and J. R. Kim, *Chem. Eng. J.*, 2017, **328**, 703–707.
- 14 C. B. Breslin, D. Branagan and L. M. Garry, *J. Appl. Electrochem.*, 2018, **49**, 195–205.
- 15 S. Menon, S. Rajeshkumar and V. Kumar, *Resour.-Effic. Technol.*, 2017, **3**, 516–527.
- 16 X. Wu, X. Xiong, G. Owens, G. Brunetti, J. Zhou, X. Yong, X. Xie, L. Zhang, P. Wei and H. Jia, *Bioresour. Technol.*, 2018, **270**, 11–19.
- 17 D. Wu, L. Huang, X. Quan and G. Li Puma, *J. Power Sources*, 2016, **307**, 705–714.
- 18 A. T. Heijne, F. Liu, R. Weijden, J. Weijma, C. J. N. Buisman and H. V. M. Hamelers, *Environ. Sci. Technol.*, 2010, **44**, 4376–4381.
- 19 X. Wu, F. Tong, X. Yong, J. Zhou, L. Zhang, H. Jia and P. Wei, *J. Hazard. Mater.*, 2016, **308**, 303–311.



Paper

- 20 S. E. P. Administration, *The Water and Wastewater Monitoring Methods*, China Environmental Science Press, Beijing, 2002.
- 21 A. Mehdinia, E. Ziaei and A. Jabbari, *Electrochim. Acta*, 2014, **130**, 512–518.
- 22 Y. Wu, X. Zhang, S. Li, X. Lv, Y. Cheng and X. Wang, *Electrochim. Acta*, 2013, **109**, 328–332.
- 23 Z. Wen, S. Ci, S. Mao, S. Cui, G. Lu, K. Yu, S. Luo, Z. He and J. Chen, *J. Power Sources*, 2013, **234**, 100–106.
- 24 I. H. Park, M. Christy, P. Kim and K. S. Nahm, *Biosens. Bioelectron.*, 2014, **58**, 75–80.
- 25 Z. He and F. Mansfeld, *Energy Environ. Sci.*, 2009, **2**, 215–219.
- 26 F. A. A. Alatraktchi, Y. Zhang and I. Angelidaki, *Appl. Energy*, 2014, **116**, 216–222.
- 27 S. Koçak and B. Aşlışen, *Sens. Actuators, B*, 2014, **196**, 610–618.
- 28 G. G. Kumar, V. G. Sarathi and K. S. Nahm, *Biosens. Bioelectron.*, 2013, **43**, 461–475.
- 29 X. Quan, B. Sun and H. Xu, *Electrochim. Acta*, 2015, **182**, 815–820.
- 30 Y. Arima and H. Iwata, *Biomaterials*, 2007, **20**, 3074–3082.
- 31 W. Xu, H. Zhang, G. Li and Z. Wu, *J. Electroanal. Chem.*, 2016, **764**, 38–44.
- 32 J. Xu, Z. Cao, Y. Zhang, Z. Yuan, Z. Lou, X. Xu and X. Wang, *Chemosphere*, 2018, **195**, 351–364.
- 33 H. C. Tao, M. Liang, W. Li, L. J. Zhang, J. R. Ni and W. M. Wu, *J. Hazard. Mater.*, 2011, **189**, 186–192.
- 34 M. Devaraj, R. Saravanan, R. Deivasigamani, V. K. Gupta, F. Gracia and S. Jayadevan, *J. Mol. Liq.*, 2016, **221**, 930–941.

